

## TECTONIC CONTROLS ON RESERVOIR PERMEABILITY IN THE DIXIE VALLEY, NEVADA, GEOTHERMAL FIELD

Stephen Hickman<sup>1</sup>, Mark Zoback<sup>2</sup>, and Richard Benoit<sup>3</sup>

<sup>1</sup>U.S. Geological Survey, 345 Middlefield Road, Menlo Park, CA 94025, U.S.A.  
hickman@theub.wr.usgs.gov

\*Department of Geophysics, Stanford University, Stanford, CA 94305, U.S.A.  
zoback@pangea.stanford.edu

<sup>3</sup>Oxbow Geothermal Corporation, 5250 South Virginia Street, Reno, NV 89502, U.S.A.  
dick\_benoit@opsi.oxbow.com

### **ABSTRACT**

To determine factors controlling permeability variations within and adjacent to a fault-hosted geothermal reservoir at Dixie Valley, Nevada, we conducted borehole televiewer observations of wellbore failure (breakouts and cooling cracks) together with hydraulic fracturing stress measurements in six wells drilled into the Stillwater fault zone at depths of 2–3 km. Measurements in highly permeable wells penetrating the main geothermal reservoir indicate that the local orientation of the least horizontal principal stress,  $S_{hmin}$ , is nearly optimal for normal faulting on the Stillwater fault. Hydraulic fracturing tests from these wells further show that the magnitude of  $S_{hmin}$  is low enough to lead to frictional failure on the Stillwater and nearby subparallel faults, suggesting that fault slip is responsible for the high reservoir productivity. Similar measurements were conducted in two wells penetrating a relatively impermeable segment of the Stillwater fault zone, located ~8 and 20 km southwest of the geothermal reservoir (wells 66-21 and 45-14, respectively). The orientation of  $S_{hmin}$  in well 66-21 is near optimal for normal faulting on the nearby Stillwater fault, but the magnitude of  $S_{hmin}$  is too high to result in incipient frictional failure. In contrast, although the magnitude of  $S_{hmin}$  in well 45-14 is low enough to lead to normal faulting on optimally oriented faults, the orientation of the Stillwater fault near this well is rotated by ~40° from the optimal orientation for normal faulting. This misorientation, coupled with an apparent increase in the magnitude of the greatest horizontal principal stress in going from the producing to nonproducing wells, acts to inhibit frictional failure on the Stillwater fault zone in proximity to well 45-14. Taken together, data from the nonproducing and producing wells thus suggest that a necessary condition for high reservoir permeability is that the Stillwater fault zone be critically stressed for frictional failure in the current stress field.

### **INTRODUCTION**

To evaluate the role of tectonic controls on the productivity of a fracture-dominated geothermal reservoir at Dixie Valley, Nevada, we are conducting an integrated study of fracturing, stress, and hydrologic properties in geothermal wells drilled into and near the Stillwater fault zone (Figure 1). This fault is a major, active, range-bounding normal fault located in the western Basin and Range province, Nevada (see Okaya and Thompson, 1985), and comprises the main reservoir for a ~62 MW geothermal electric power plant operated by Oxbow Geothermal Corporation. Although earthquakes have not ruptured this segment of the Stillwater fault in historic times, large ( $M = 6.8-7.7$ ) earthquakes have occurred within the past 80 years along range-bounding faults both to the northeast and southwest of the Dixie Valley Geothermal Field (DVGF), and geologic evidence shows that the Stillwater fault abutting the DVGF experienced two or more faulting episodes (total offset ~9 m) during the past 12,000 years (Wallace and Whitney, 1984).

The principal goal of this study is to define the nature, distribution, and hydraulic properties of fractures associated with the DVGF, and to characterize the manner in which these fractures, and hence the overall reservoir hydrology, are related to the local stress field. This project was initiated in late 1995 with an extensive downhole measurements program conducted in a 2.6-km-deep geothermal production well (well 73B-7) drilled into the Stillwater fault zone by Oxbow Geothermal Corporation (see Hickman and Zoback, 1997; Barton et al., 1997; Hickman et al., 1997). This study has since been expanded to include borehole televiewer logging, temperature/pressure/spinner (TPS) logging, and hydraulic fracturing stress measurements from additional wells within the primary zone of geothermal production (transmissivities on the order of  $1 \text{ m}^2/\text{min}$ ) and from wells within a few km of the producing zone that

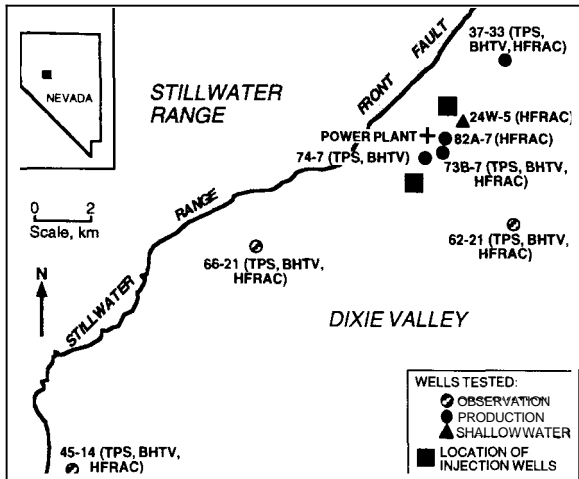


Fig. 1 Map showing geothermal wells in Dixie Valley, Nevada. Injection and production wells penetrated highly permeable portions of the southeast-dipping Stillwater fault zone, whereas observation wells failed to encounter enough permeability to be of commercial value. Measurements made in these wells included TPS: Temperature/pressure/spinner logs; BHTV: borehole televiwer logs; HFRAC: Hydraulic fracturing stress measurements.

were relatively impermeable and, hence, not commercially viable (transmissivities of about  $10^{-4}$  m<sup>2</sup>/min). The results from stress measurements and observations of wellbore failure in these wells are presented below. Analyses of borehole logs for the geometrical and hydrologic properties of individual fractures and whole-well hydrologic properties are presented by Barton et al. (this volume) and Morin et al. (this volume), respectively.

The measurements made in these wells make possible a systematic, comparative study of the effects of in situ stress on fracture permeability along producing and nonproducing segments of the Stillwater fault zone. By comparing and contrasting data from both productive and nonproductive wells, it should be possible to determine if a relationship exists between the contemporary in-situ stress field and reservoir productivity. If so, then these types of data will provide a valuable tool for geothermal reservoir exploration by allowing one to determine which faults or fault segments are likely to be hydraulically conductive in a given stress field. Furthermore, these data would provide critical input on decisions related to redrilling of impermeable (i.e., "dry") wells or abandonment of an area or prospect. At some future date, it is also hoped these methods can be used to locate and engineer future production and injection wells and to design enhanced recovery programs (e.g., massive hydraulic fracturing) for less-than-commercial wells within existing geothermal reservoirs.

## METHOD

The geometry and orientation of drilling-induced tensile fractures and borehole breakouts (see below) were determined using borehole televiwer (BHTV) logs. The BHTV is a wireline logging tool that provides a continuous, oriented, ultrasonic image of a borehole wall (see Zemanek et al., 1970). The high temperatures encountered in these wells (up to  $\sim 240^\circ\text{C}$ ) required the use of specialized televiwer tools, owned by Stanford University and the US Geological Survey. These tools were repeatedly calibrated at the surface for orientation and ultrasonic travel times in specially designed calibration tanks and repeat logging runs were used to provide independent checks on the orientations of the images obtained. Data were digitized from the magnetic field tapes and then processed to remove noise, stick-slip effects and other tool-related problems.

Although hydraulic fracturing stress measurements are typically conducted in short intervals of open hole using inflatable rubber packers, high borehole temperatures precluded the use of packers in these wells (see Hickman et al., 1988, for discussion of the hydraulic fracturing technique and the interpretation methods used here). Instead, the hydraulic fracturing tests in this study were either conducted in short pilot holes during drilling of a new geothermal production well or in an open-hole section of an already drilled and cased well. In the first type of test, following cementation and pressure testing of each casing string, 15- to 30-m-long pilot holes were drilled out the bottom of the well and the entire casing string was pressurized to induce a hydraulic fracture in the uncased pilot hole. Repeated pressurization cycles were then employed to extend this fracture away from the borehole. In the second type of test, the entire borehole – including 2 to 3 km of cased hole plus up to 800 m of open hole – was pressurized during the hydraulic fracturing test and a TPS log was conducted during the last cycle of the test to identify the depth at which the hydraulic fracture was created. Although necessitated by high borehole temperatures, both types of tests also resulted in more rapid, and hence less expensive, in-situ stress testing than would have been the case had drill-pipe deployed packers been used.

Pressures and flow rates were measured at the surface and temperature-compensated pressure gauges were suspended a few meters above the test interval to record downhole pressure during each test. The magnitude of the minimum horizontal principal stress,  $S_{hmin}$ , was determined from the instantaneous shut-in pressure (ISIP), or the pressure at which the pressure-time curve departs from an initial linear pressure drop immediately after the pump is turned off and the well is shut in (Figure 2). Pressures recorded during a stepwise change in flow rate during

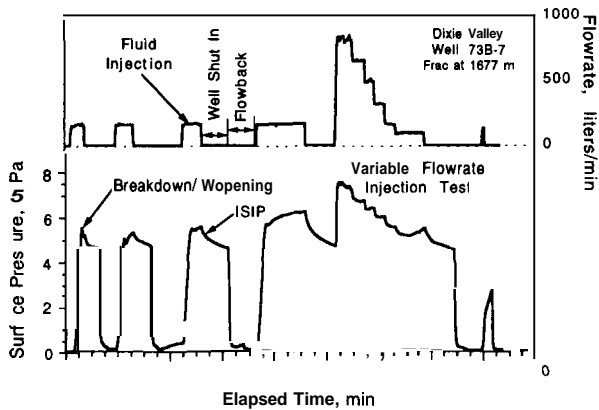


Fig. 2 Surface pressure and flow rate records from the hydraulic fracturing test conducted at 1663–1690 m depth in well 73B-7. Pressures were also recorded using a downhole temperature-compensated pressure transducer suspended a few meters above the test interval.

the last pumping cycle of each test were used to detect changes in the permeability of the test interval resulting from closure of the hydraulic fracture and provided an additional constraint on the magnitude of  $S_{hmin}$ .

In a hydraulic fracturing test the magnitude of the maximum horizontal principal stress,  $S_{Hmax}$ , is typically determined utilizing a fracture initiation, or breakdown, criteria for pure tensile fractures initiating in intact rock along the  $S_{Hmax}$  direction. In these wells, however, BHTV logs conducted before the hydraulic fracturing tests showed that the tested intervals contained numerous preexisting fractures (both natural and drilling-induced) at a variety of orientations (see below and Barton et al, this volume). Thus, it was not possible to directly measure the magnitude of  $S_{Hmax}$  during these tests. However, as discussed below, bounds to the magnitude of  $S_{Hmax}$  were obtained using estimates of compressive rock strength and the presence or absence of borehole breakouts in these wells.

The vertical (overburden) stress,  $S_v$ , was calculated using geophysical density logs conducted in the test wells, or nearby wells, in conjunction with rock densities measured on surface samples obtained from Dixie Valley (Okaya and Thompson, 1985).

## RESULTS AND DISCUSSION

We have conducted BHTV and/or hydraulic fracturing stress measurements in a total of eight wells at Dixie Valley (Figure 1). With the exception of a 550-m-deep water well drilled ~1 km northeast of well 73B-7 (well 24W-5) and a 3.4-km-deep observation well (62-21) drilled toward the center of Dixie Valley, all of these wells penetrate the Stillwater fault zone at depths of 2 to 3 km. Four of these wells (73B-7,

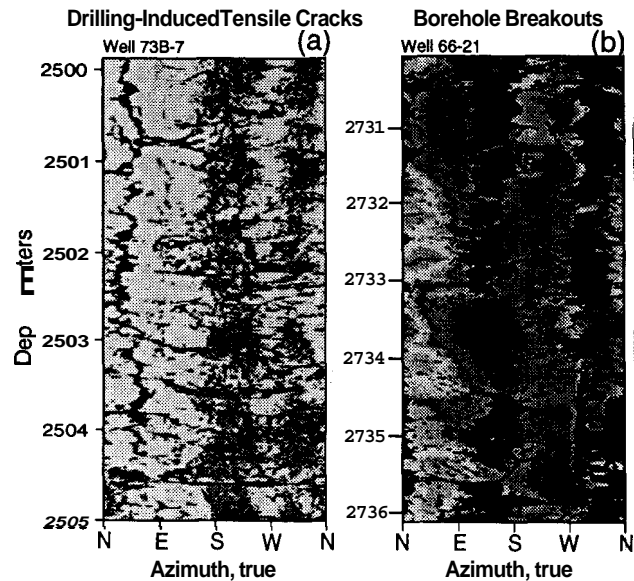


Fig. 3 (a) BHTV log from well 73B-7 showing drilling-induced (cooling) fractures, imaged as undulating vertical features occurring on diametrically opposed sides of the borehole and aligned in a northeast-southwest direction. (b) BHTV log from well 66-21 showing the development of stress-induced breakouts (discontinuous dark bands).

82A-7, 74-7 and 37-33) penetrated the highly permeable (i.e., producing) segment of the fault zone constituting the main geothermal reservoir. The other two wells (66-21 and 45-14), which failed to encounter enough permeability to be viable production wells, penetrated segments of the Stillwater fault zone located approximately 8 and 20 km southwest of the main reservoir.

### Producing Fault Segment

BHTV logs from well 73B-7 revealed extensive drilling-induced tensile fractures (e.g., Figure 3a). As discussed by Moos and Zoback (1990), these cracks result from the superposition of a tensional circumferential thermal stress induced by circulation of relatively cold drilling fluids and the concentration of ambient tectonic stresses at the borehole wall. As these tensile cracks should form perpendicular to the azimuth of the minimum horizontal principal stress, they indicate that the direction of  $S_{hmin}$  in well 73B-7 is  $N57^{\circ}W \pm 10^{\circ}$  (see Hickman and Zoback, 1997).

Tensile (cooling) cracks were also observed in wells 74-7 and 37-33, but they were less extensively developed than in well 73B-7 and their interpretation is more ambiguous. The distribution of tensile crack orientations in well 74-7 is bimodal, being aligned in a  $N72^{\circ}E$  direction in the silicic tuff at 2580–2640 m depth and  $N38^{\circ}E$  in gabbro and anorthosite (the Humbolt Lopolith) at 2640–2680 m. As the

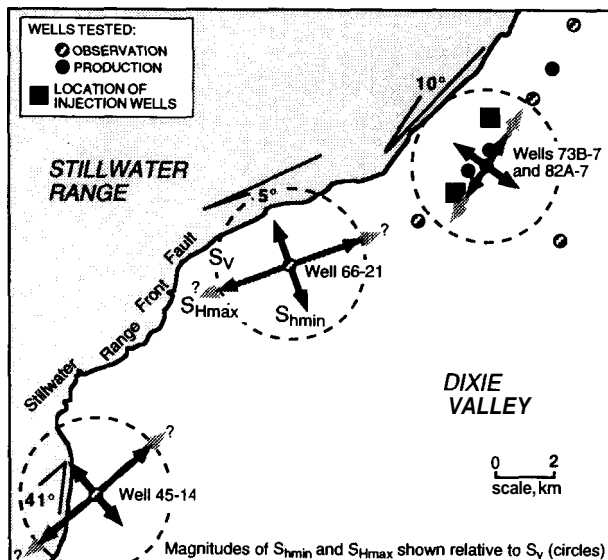


Fig. 4 Orientations and relative magnitudes of the least horizontal principal stress,  $S_{hmin}$ , and the greatest horizontal principal stress,  $S_{Hmax}$ , at Dixie Valley. The length of each arrow is proportional to the magnitude of the corresponding stress, normalized to the magnitude of the vertical stress  $S_v$  (dashed circle) appropriate for that well and test depth (all stresses are compressive). Lower and upper bounds on  $S_{Hmax}$ , determined through analysis of conditions for breakout formation, are depicted as dark and light gray arrows, respectively. Stresses shown for wells 73B-7 and 82A-7 are average values from three measurements at 1.7 to 2.5 km depth. Also shown is the extent (in degrees) to which the Stillwater fault is locally deviated from the optimal orientation for normal faulting. As the Stillwater fault outcrops at nearly constant elevation, the fault trace shown (solid black line) closely approximates the subsurface fault strike.

Humbolt Lopolith contains all of the producing fractures encountered in this well, we consider the corresponding  $S_{hmin}$  direction ( $N52^\circ W$ ) to be the most representative of the state of stress within the main geothermal reservoir at this site. Tensile cracks were encountered in well 37-33 within 150 m of the primary fluid-producing zone, but these cracks change orientation by up to  $90^\circ$  over only a few tens of meters. We interpret these orientation changes to result from highly localized perturbations to the in-situ stress field, perhaps resulting from slip on nearby fractures (see Barton and Zoback, 1994), rendering these features unreliable as tectonic stress direction indicators. No stress direction indicators were observed in BHTV logs from well 62-21; and BHTV logs were unsuccessful in well 82A-7 due to hole conditions. Taken together, tensile fractures from well 73B-7 and the lower portion of well 74-7 indicate that

the direction of  $S_{hmin}$  adjacent to the highly permeable segment of the Stillwater fault is about  $S55^\circ E \pm 15^\circ$ . As the Stillwater fault at this location dips  $S45^\circ E$  at  $\sim 53^\circ$ , it is nearly at the optimal orientation for normal faulting in the current stress field (Figure 4).

Analysis of hydraulic fracturing tests from the deep geothermal production wells 73B-7 and 82A-7, together with the shallow water well 24W-5 (see Figure 1), shows that the magnitude of  $S_{hmin}$  is very low relative to the calculated vertical stress, with  $S_{hmin}/S_v$  ranging from 0.45 to 0.62 at depths of 0.4–2.5 km (Figure 5a). Stress measurements made near the bottoms of wells 73B-7 and 82A-7 indicate that  $S_{hmin}/S_v$  reaches its lowest values of 0.45 to 0.51 within a few hundred meters of the Stillwater fault zone. A single stress measurement conducted in the relatively impermeable well 62-21, which was adjacent to the primary producing segment of the Stillwater fault but located near the center of Dixie Valley (Figure 1), yielded an  $S_{hmin}/S_v$  value of about 0.56 at a depth of 2.9 km (Figure 5b).

An extensive stress measurement program was also conducted during drilling of production well 37-33, located about 4 km northeast of the geothermal power plant (Figure 1). A total of five stress measurements were attempted in this well, only three of which actually succeeded in inducing hydraulic fractures (Figure 5c). The remaining two tests were terminated when the maximum safe wellhead pressure ( $-12.4$  MPa) was reached, yielding lower bounds to the magnitude of  $S_{hmin}$ . These lower bounds, together with a successful hydraulic fracturing test at 1888 m, revealed relatively high  $S_{hmin}/S_v$  values of 0.74 or greater at depths of 1.57 to 1.89 km. The cause for these anomalously high  $S_{hmin}$  magnitudes is unknown, although it could be due to localized relief of differential stress (i.e.,  $S_v - S_{hmin}$ ) accompanying small-magnitude earthquakes or slip events on faults basin-ward of the main Stillwater fault zone. It is important to note, however, that the deepest stress measurement in well 37-33, which was conducted directly above the Stillwater fault zone, yielded  $S_{hmin}$  magnitudes comparable to those observed in the other producing wells immediately to the southwest, with an  $S_{hmin}/S_v$  value of 0.46 at a depth of 2.63 km.

Given the absence of borehole breakouts in the BHTV logs from the producing wells, upper bounds to the magnitude of  $S_{Hmax}$  were obtained using  $S_{hmin}$  magnitudes measured in well 73B-7 together with theoretical models for breakout formation. These models (see Moos and Zoback, 1990) predict that borehole breakouts will initiate along the azimuth of  $S_{hmin}$  whenever the maximum effective circumferential stress,  $\sigma_{\theta\theta}^{max}$ , at the borehole wall exceeds the compressive rock strength,  $C_o$ ; i.e.:

$$\sigma_{\theta\theta}^{max} = 3S_{Hmax} - S_{hmin} - P_p - P_m \geq C_o \quad (1)$$

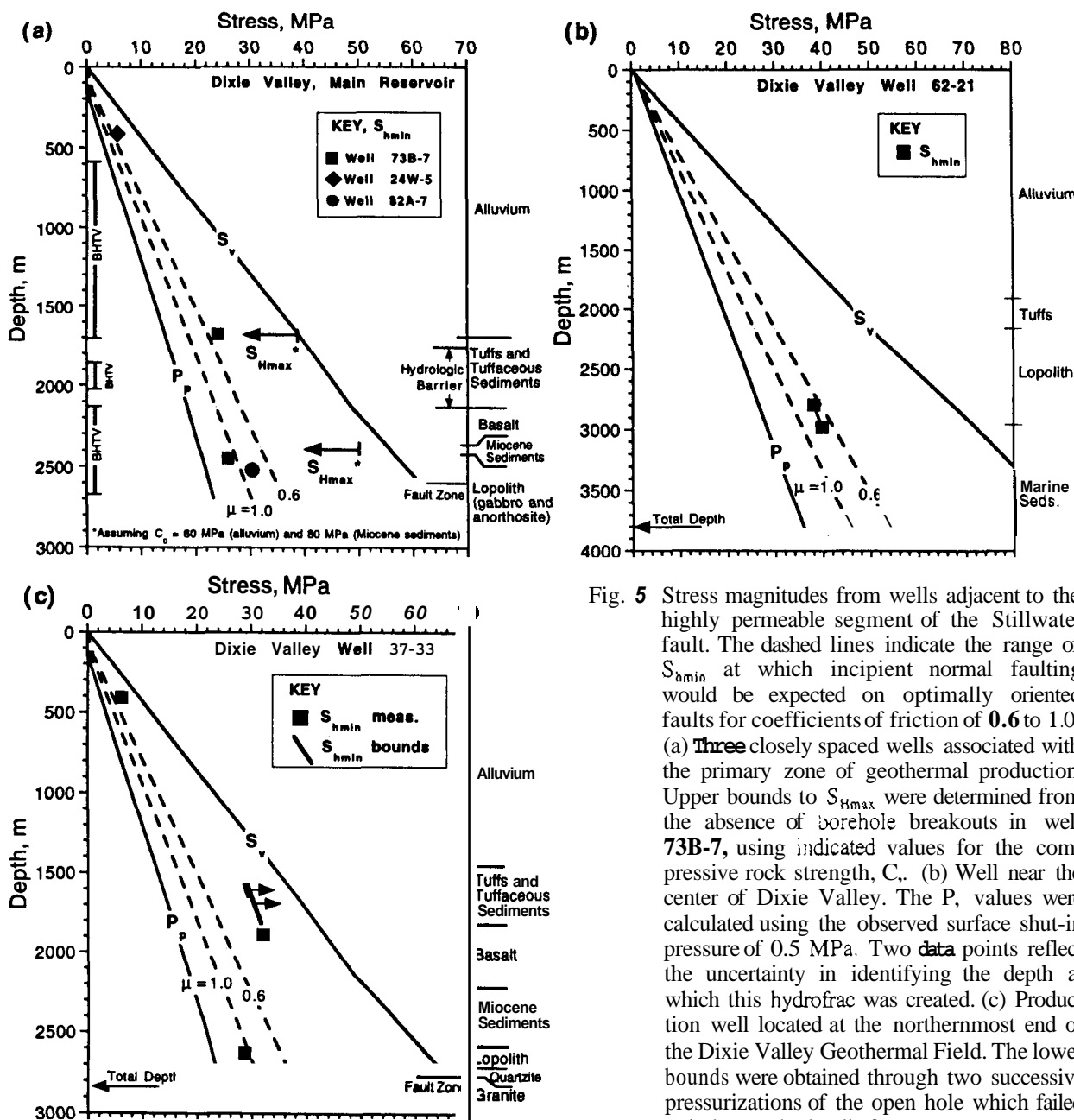


Fig. 5 Stress magnitudes from wells adjacent to the highly permeable segment of the Stillwater fault. The dashed lines indicate the range of  $S_{hmin}$  at which incipient normal faulting would be expected on optimally oriented faults for coefficients of friction of 0.6 to 1.0. (a) Three closely spaced wells associated with the primary zone of geothermal production. Upper bounds to  $S_{Hmax}$  were determined from the absence of borehole breakouts in well 73B-7, using indicated values for the compressive rock strength,  $C_r$ . (b) Well near the center of Dixie Valley. The  $P_r$  values were calculated using the observed surface shut-in pressure of 0.5 MPa. Two data points reflect the uncertainty in identifying the depth at which this hydrofrac was created. (c) Production well located at the northernmost end of the Dixie Valley Geothermal Field. The lower bounds were obtained through two successive pressurizations of the open hole which failed to induce a hydraulic fracture.

where  $P_r$  is the formation pore pressure and  $P_d$  is the mud pressure exerted on the borehole wall during drilling. Ideally, laboratory failure tests should be conducted on the same rocks penetrated by the well to determine the appropriate value for  $C_r$  to use in Equation 1. Although we hope to conduct such tests in the future, such data are not yet available for the rock types penetrated by well 73B-7. Instead, we estimated  $C_r$  based upon published compilations of the compressive strength of rocks of similar lithology (Lockner, 1995). This analysis requires that  $S_{Hmax}$  be less than or equal to  $S_v$  at depths of 1.7 and 2.4 km, indicating a normal faulting stress regime (Figure 5a).

Since the  $S_{hmin}$  azimuths determined in well 73B-7 and the lower portion of 74-7 indicate that the Stillwater fault is nearly at the optimal orientation for normal faulting (see Figure 4), stress magnitudes from the hydraulic fracturing tests in the producing wells can be analyzed in terms of the potential for slip on this and other (subparallel) faults. In accordance with the Coulomb failure criterion, frictional failure (i.e., normal faulting) would occur at a critical magnitude of  $S_{hmin}$  given by (Jaeger and Cook, 1976):

$$S_{hmin\ crit} = (S_v - P_p) / [(\mu^2 + 1)^{1/2} + \mu]^2 + P_p \quad (2)$$

where  $\mu$  is the coefficient of friction of preexisting

faults. It is assumed here that  $\mu$  ranges from 0.6 to 1.0, in accord with laboratory sliding experiments (after Byerlee, 1978). Estimates of undisturbed (i.e., preproduction) formation fluid pressure were obtained assuming that  $P_p$  was in hydrostatic equilibrium with the water table at 152 m depth by integrating water density as a function of pressure and temperature (from Keenan et al., 1978), as appropriate to ambient geothermal conditions, and including a small correction for total dissolved solids. Pressure logs conducted in deep ( $\leq 2.7$  km) wells drilled into the Stillwater fault zone and adjacent rocks prior to commencement of large-scale geothermal production about ten years ago indicate that this  $P_p$  is accurate to within 0.5 MPa for units penetrated by the production wells below about 250 m.

In this manner, one can calculate the range of  $S_{hmin}$  magnitudes at which normal faulting would be expected along the producing segment of the Stillwater fault zone (Figures 5a and c). This analysis indicates that  $S_{hmin}$  at depths of 2.4 to 2.6 km in the southern producing wells (Figure 5a) and at a depth of approximately 2.7 km in well 37-33 (Figure 5c) is low enough to result in incipient normal faulting on the Stillwater and other nearby subparallel faults (i.e.,  $S_{hmin}$  is less than predicted by Equation 2 for  $\mu = 0.6$ ). Similar results were obtained from the "background" well 62-21 (Figure 5b), indicating that the near-failure stress state adjacent to the permeable segment of the Stillwater fault zone is relatively homogeneous.

Permeability reduction and the establishment of fault seals would be expected along the productive segment of the Stillwater fault, given the high reservoir temperatures ( $\sim 220$ – $250^\circ$  C at 2.3–3.0 km); surface observations of hydrothermal alteration, mineralization, and pressure-solution deformation within and adjacent to the fault zone (e.g., Seront et al., 1997); and thermal evidence for upward transport of hydrothermal fluids within the fault zone (Benoit, 1996; Williams et al., 1997). In particular, analyses of fluid samples recovered from the Stillwater fault zone prior to reservoir production by Oxbow Geothermal Corporation indicate a decrease in silica concentration of about 120 ppm as these fluids ascend from 3.0 to 2.3 km. This loss of silica can be expected to seal fractures within the Stillwater fault zone over geological time scales, thereby reducing the high overall fault-zone permeability. However, the observation that the permeability of fractures within and adjacent to the highly productive segment of the Stillwater fault zone is quite high (see Morin et al., this volume) and that these fractures are favorably aligned and critically stressed for normal faulting in the current stress field (Barton et al., this volume) suggests that dilatancy associated with ongoing fault slip in response to high differential stresses (i.e.,  $S_1 - \sigma_3$ ) is sufficient to counteract the expected permeability reduction.

### Nonproducing Fault Segment

Similar data were collected in the two wells (66-21 and 45-14) penetrating relatively impermeable segments of the Stillwater fault zone (Figure 1). Unlike wells adjacent to the productive fault segment, BHTV logs from both of these wells showed the intermittent development of stress-induced borehole breakouts over much of the logged intervals (Figure 3b; see also Figure 6). These breakouts indicate that the direction of  $S_{hmin}$  in wells 66-21 and 45-14 is  $N20^\circ W \pm 20^\circ$  and  $N41^\circ W \pm 12^\circ$ , respectively (Figure 4). It is important to note that a short (5-m-long) interval of cooling cracks was also observed in well 45-14 and that the orientation of  $S_{hmin}$  inferred from these cracks and from breakouts in the same well agree to within  $5^\circ$ . Even though the  $S_{hmin}$  direction measured in well 66-21 is significantly different from that observed in the producing wells to the northeast, it is still nearly perpendicular to the local strike of the Stillwater fault zone, indicating that the fault at this location is optimally oriented for normal faulting. In contrast, stress orientations from well 45-14 are similar to those observed in the producing wells, even though the local strike of the fault differs by about  $40^\circ$  (Figure 4). Thus, the Stillwater fault adjacent to this southernmost well is severely missoriented for normal faulting in the present stress field.

A single hydraulic fracturing stress measurement was conducted in each of these nonproducing wells (Figures 6a and b). TPS logs collected during the final cycles of these tests show that these hydrofractures were induced just below the casing of wells 66-21 and 45-14. These tests indicate that  $S_{hmin}/S_v$  adjacent to the nonproducing segment of the Stillwater fault ranges from 0.55 to 0.64 at depths of 1.9 to 2.2 km, which is higher than the values of 0.45 to 0.51 observed at 2.4 to 2.6 km depth in producing wells to the northeast.

Since breakouts were present in wells 66-21 and 45-14, we used Equation 1 to place lower bounds on the corresponding magnitude of  $S_{Hmax}$ . In so doing, we extrapolated our measurements of  $S_{hmin}$  magnitudes in these wells to the depths at which breakouts were observed (assuming constant  $S_{hmin}/S_v$ ) and used a range of estimates for the compressive strength of rock types encountered at these depths (after Lockner, 1995). We thus determined that the magnitude of  $S_{Hmax}$  in these nonproductive wells is greater than or equal to  $S_1$  (Figure 6). This is in marked contrast to wells penetrating the permeable main reservoir, where  $S_{Hmax}$  is less than  $S_v$  (Figure 5a).

As was done for wells adjacent to the permeable fault segment, we used Equation 2 to determine the proximity of nearby optimally oriented normal faults to Coulomb failure. Interestingly, fluid pressures in wells 66-21 and 45-14 are artesian, in contrast to the

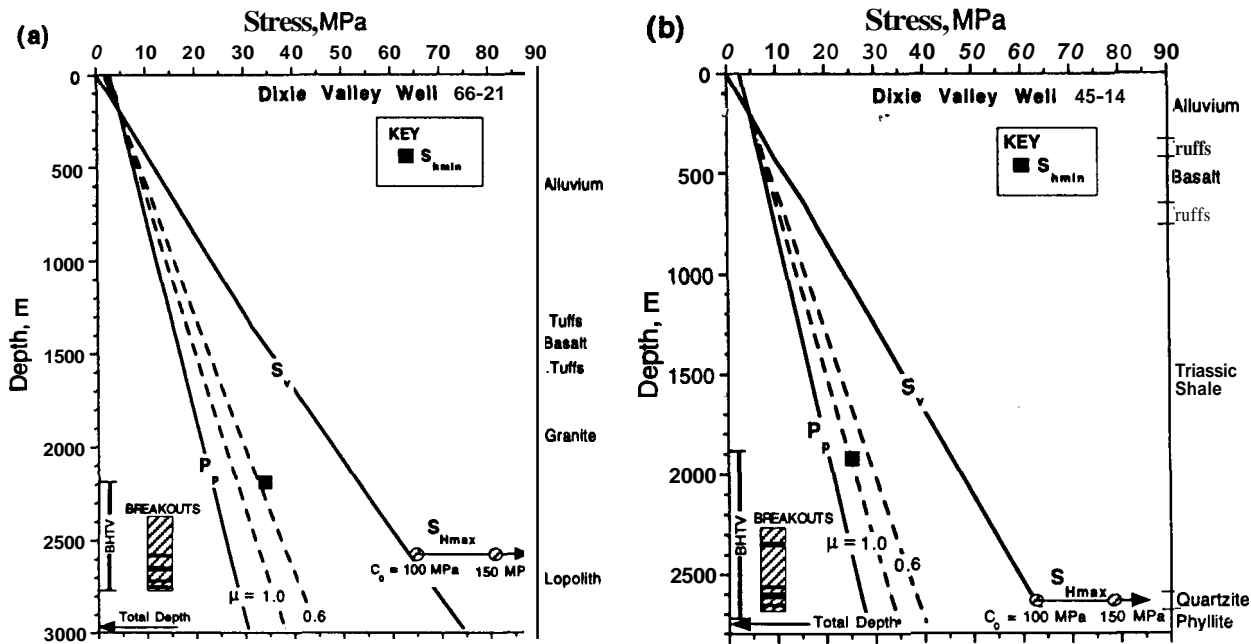


Fig. 6 Same as Fig. 5, but for wells adjacent to the relatively impermeable segment of the Stillwater fault zone, located 8 and 20 km southwest of the main geothermal reservoir (see Fig. 1). Also shown are the depth extent of BHTV logging coverage and the distribution of breakouts in each well; breakouts were either discontinuous (hatched pattern) or continuous (solid lines). Lower bounds to  $S_{Hmax}$  were obtained using a breakout initiation criteria and estimates of  $C_o$ . In this analysis we assumed that  $C_o$  was equal to 100 or 150 MPa for the Humboldt Lopolith (gabbro and anorthosite) and quartzite, although the actual value of  $C_o$  could be much higher (see Lockner, 1995).

subhydrostatic pressures encountered in wells penetrating the main geothermal reservoir. Although the static fluid pressure within the Stillwater fault zone at these locations is not well known, the long-term well-head shut-in pressure for well 66-21 is  $-2.7$  MPa and we have used this value as the datum in calculating  $P_p$  at depth for both of these sites (see Figure 6). For well 66-21, this analysis indicates that the magnitude of  $S_{hmin}$  is not quite low enough to induce frictional failure (Figure 6a). Thus, the Stillwater and subparallel faults are optimally oriented – but not critically stressed – for normal faulting.

In contrast, application of Byerlee's Law to well 45-14 indicates that  $S_{hmin}$  at this site is low enough to result in incipient frictional failure on optimally oriented normal faults (Figure 6b). Indeed, Coulomb failure analysis performed on individual fractures in this well (Barton et al., this volume) indicates that some – but not all – of the hydraulically conductive fractures encountered in this well are critically stressed for frictional failure. However, as shown by Barton et al. (this volume) the combined effects of an increase in  $S_{Hmax}$  magnitudes relative to  $S_v$ , and the extreme misorientation of the Stillwater fault zone with respect to the principal stress directions near well 45-14 (Figure 4), lead to a decrease in the proximity of the Stillwater fault zone itself to Coulomb failure at this site. This observation, together with our analysis

indicating that the magnitude of  $S_{hmin}$  in well 66-21 is too high to result in incipient normal faulting (even on optimally oriented faults), suggests that a necessary condition for high reservoir permeability is that both the local state of stress and the orientation of the Stillwater fault zone be such that the fault is critically stressed for frictional failure.

## CONCLUSIONS

Hydraulic fracturing stress measurements and observations of borehole wall failure to depths of 3.0 km indicate that in-situ stresses are of the appropriate magnitude and orientation for frictional failure (i.e., normal faulting) on the highly permeable segment of the Stillwater fault zone constituting the principal reservoir for the Dixie Valley Geothermal Field. Specifically, the magnitude of the least horizontal principal stress determined within a few hundred meters of the primary producing zones in these wells is in accord with simple frictional faulting theory assuming laboratory-derived coefficients of friction of 0.6 to 1.0 and estimates of the in-situ fluid pressure that existed prior to large-scale geothermal production. In contrast, similar measurements made in wells drilled into nonproductive (i.e., relatively impermeable) segments of the Stillwater fault zone southwest of the main reservoir indicate that these fault segments are not critically stressed for frictional

failure in the current stress field. Thus, in-situ measurements of stress orientations and magnitudes in proximity to fault-hosted geothermal reservoirs can help indicate which faults or fault segments might be viable candidates for geothermal production.

### **ACKNOWLEDGMENTS**

This work was supported by the U.S. Department of Energy (DOE) Geothermal Technologies Program. However, any opinions, findings, conclusions, or recommendations expressed herein are those of the authors and do not necessarily reflect the views of the DOE. Additional support was provided by the Earthquake Hazards Reduction Program of the U.S. Geological Survey.

### **REFERENCES**

- Barton, C.A., and M.D. Zoback (1994), "Stress Perturbations Associated with Active Faults Penetrated by Boreholes: Possible Evidence for Near-Complete Stress Drop and a New Technique for Stress Magnitude Measurements", *Journal of Geophysical Research*, **99**, 9373-9390.
- Barton, C.A., S. Hickman, R.H. Morin, M.D. Zoback, T. Finkbeiner, J. Sass, and R. Benoit (1997), "Fracture permeability and its relationship to in-situ stress in the Dixie Valley, Nevada, geothermal reservoir", *Proceedings 22nd Workshop on Geothermal Reservoir Engineering*, Stanford Univ., Stanford, CA, 147-152.
- Benoit, W.R. (1996), "Injection of geothermal fluid in Nevada as typified by the Dixie Valley project", in *Deep Injection Disposal of Hazardous and Industrial Wastes*, J. Apps and C.-F. Tsang (eds.), Academic Press, San Diego, pp. 449-464.
- Byerlee, J.D. (1978), "Friction of rocks", *Pure and Applied Geophysics*, **116**, 615-629.
- Hickman, S., and M.D. Zoback (1997), "In-situ stress in a fault-hosted geothermal reservoir at Dixie Valley, Nevada", *Proceedings 22nd Workshop on Geothermal Reservoir Engineering*, Stanford Univ., Stanford, CA, pp. 141-146.
- Hickman, S., M.D. Zoback, and J.H. Healy (1988), "Continuation of a deep borehole stress measurement profile near the San Andreas Fault, I: Hydraulic fracturing stress measurements at Hi Vista, Mojave Desert, CA", *Journal of Geophysical Research*, **93**, 15183-15195.
- Hickman, S., C.A. Barton, M.D. Zoback, R. Morin, J. Sass, and R. Benoit (1997), "In situ stress and fracture permeability in a fault-hosted geothermal reservoir at Dixie Valley, Nevada", *Transactions Geothermal Resources Council*, **21**, Burlingame, CA, pp.181-189.
- Jaeger, J.C., and N.G.W. Cook (1976), *Fundamentals of Rock Mechanics*, 2nd ed., **585** pp., Chapman and Hall, London.
- Keenan, J.H., F.G. Keyes, P.G. Hill, and J.G. Moore (1978), *Steam Tables: Thermodynamic Properties of Water Including Vapor, Liquid, and Solid Phases*, John Wiley & Sons, New York, 156 pp.
- Lockner, D.A. (1995), "Rock Failure", in *Rock Physics and Phase Relations: A Handbook of Physical Constants*, T. Ahrens (ed.), American Geophysical Union, Washington, DC, pp. 127-147.
- Moos, D., and M.D. Zoback (1990), "Utilization of observations of well bore failure to constrain the orientation and magnitude of crustal stresses: Application to continental, Deep Sea Drilling Project, and Ocean Drilling Program boreholes". *Journal of Geophysical Research*, **95**, 9305-9325.
- Okaya, D.A., and G. Thompson (1985), "Geometry of Cenozoic extensional faulting: Dixie Valley, Nevada", *Tectonics*, **4**, 107-125.
- Seront, B., T.-f. Wong, J.S. Caine, C.B. Forster, and J.T. Fredrich (1998), "Laboratory characterization of hydromechanical properties of a seismogenic normal fault system", *Journal of Structural Geology* (in press).
- Wallace, R.E., and R.A. Whitney (1984), "Late Quaternary history of the Stillwater seismic gap, Nevada", *Bulletin of the Seismological Society of America*, **74**, 301-314.
- Williams, C.F., J.H. Sass, and F.V. Grubb (1997), "Thermal signature of subsurface fluid flow in the Dixie Valley geothermal field, Nevada", *Proceedings 22nd Workshop on Geothermal Reservoir Engineering*, Stanford Univ., Stanford, CA, pp. 161-168.
- Zemanek, J., E. E. Glenn, L. J. Norton, and R. L. Caldwell, (1970), "Formation evaluation by inspection with the borehole televiwer", *Geophysics*, **35**, 254-269.